PHYSICAL REVIEW B VOLUME 50, NUMBER 3 15 JULY 1994-I

Optical studies of locally implanted magnetic ions in GaAs

J. M. Kikkawa, J. J. Baumberg, and D. D. Awschalom
Department of Physics, University of California, Santa Barbara, California 93106

D. Leonard and P. M. Petroff
Department of Materials and Electrical and Computer Engineering, University of California, Santa Barbara, California 93106
(Received 23 March 1994)

We report the development of a Mn^{2+} focused ion beam for use in the direct fabrication of submicrometer magnetic structures. Mn-implanted GaAs bulk epilayers and quantum wells are studied by low-temperature cathodoluminescence and polarization-resolved photoluminescence. The data demonstrate that Mn ions are magnetically active, producing optical polarizations of 70% at 8 T.

Renewed interest in the study of magnetism has been stimulated by recent advances in materials science that have uncovered interesting spin-dependent phenomena in both transport and optical properties. This is typified by the advent of epitaxially grown II-VI diluted magnetic semiconductors which show enhanced Zeeman splittings of the electronic bands, enabling the design of magnetically tunable spin-dependent heterostructures that possess strongly circularly polarized luminescence, giant Faraday rotations, and carrier spin segregation to different layers.[1] Recent experiments have shown that despite low Mn solubility in III-V compounds, significant concentrations can be incorporated into epitaxial layers through careful control of growth conditions.[2,3] In addition, the deposition of Mn with a III/V element can yield binary films which are ferromagnetic.[4] Here we introduce a method for integrating magnetic impurities using focused ion beam (FIB) implantation of Mn ions. FIB resolutions of ~ 100 nm allow direct submicrometer patterning of magnetic properties which can be done in conjunction with molecular-beam-epitaxy (MBE) growth of quantum structures, facilitating device integration and simplifying processing. In this study, cathodoluminescence and magneto-optical measurements of Mn^{2+}-implanted GaAs structures demonstrate that such FIB implants are magnetically active in GaAs. Large photoluminescence polarizations exceed predictions based on independent magnetic spins, suggesting that alternate models be considered.

In order to study implantation of Mn^{2+} into both bulk GaAs and quantum-well (QW) structures, we use two distinct samples grown by MBE on undoped (100) GaAs substrates. For bulk measurements, the first design incorporates a 4000-Å GaAs epilayer clad by 200-Å $Al_{0.3}Ga_{0.7}As$ barriers, grown on a 5000-Å GaAs buffer and capped by 100 Å of GaAs. The cladding barriers prevent the escape of excited carriers to the surface or substrate. In the second design, a QW stack allows us to explore magnetic properties of GaAs:Mn in quantum confined geometries and to monitor the depth of the implanted ions. Starting with an 800-Å smoothing superlattice and 500 Å of $Al_{0.3}Ga_{0.7}As$, a series of six different GaAs wells (in order 200, 100, 50, 140, 70, and 35 Å) are spaced by 1000-Å $Al_{0.3}Ga_{0.7}As$ barriers. This is followed by 500 Å of $Al_{0.3}Ga_{0.7}As$ and a 200-Å GaAs capping layer. We denote these structures the bulk GaAs sample and the QW sample, respectively.

Samples are locally implanted with Mn^{2+} using a 150-kV FIB operating with a recently designed liquid-metal-ion source (LMIS). The LMIS is prepared by melting a Sn/Mn (60/40 by weight) alloy onto a tungsten filament and heater coil assembly under a 10^{-5}-Torr vacuum. During implantation, the heater coil liquifies the alloy, from which ions are field-emitted, passed through an $E \times B$ mass filter, and subsequently accelerated and focused onto the target. While the emission yields both Mn_{55}^{+} and Mn_{55}^{2+} (in addition to isotopes of Sn^{+}, Sn^{2+}, and various molecular ions), Mn^{+} cannot be reliably separated from Sn_{112}^{2+} due to their similar charge-to-mass ratios. Thus we use Mn^{2+} throughout this study, although it is ten times less abundant than Mn^{+}, at a maximum current density of 0.2 A/cm^2.

The patterns consist of 50×50 μm^2 squares implanted at energies between 50 and 200 keV and at doses of 10^{11}–10^{15} ions/cm^2. Uniform coverage is achieved by rastering the submicrometer spot over the desired area. Patterns are arranged in a 3×5 array (inset, Fig. 1), and four identical arrays are written on each structure which is then cleaved to obtain four separate samples. In order to reduce lattice damage and improve the optical quality, rapid thermal annealing (RTA) is performed in an inert forming gas of 90% N_2 and

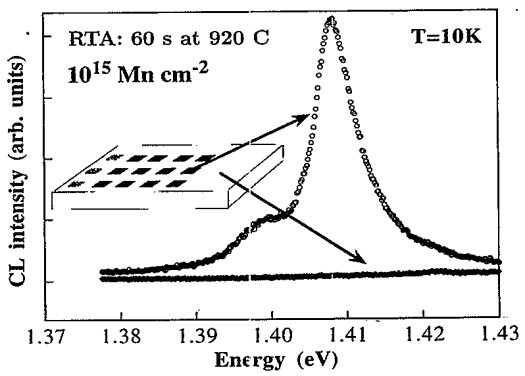

FIG. 1. Cathodoluminescence spectra from unimplanted and 10^{15} Mn cm^{-2}, 100-keV Mn^{2+} FIB patterned areas of the bulk GaAs sample after annealing at 920 °C for 60 s.

10% H_2 under a GaAs cover. For each structure we anneal three samples for 5 s at 850 °C, 20 s at 900 °C and 60 s at 920 °C, while leaving the fourth unannealed. Finally, the entire sample preparation is repeated using Ga^+ ions as a nonmagnetic control.

Low-temperature cathodoluminescence (CL) spectroscopy is used to image the spatial variations in luminescence arising from FIB patterning and to monitor the effects of annealing. Samples are placed in a modified electron microscope and kept at $T\sim 10$ K by thermal contact with circulating liquid helium. Excitation by a 120-keV electron beam at a current of 10 nA and a spot size of 15 nm produces luminescence which is collected by an ellipsoidal mirror and optical fiber bundle, passed through a monochromator, and detected by a cooled GaAs photomultiplier tube. Figure 1 contrasts the CL spectra obtained within the implanted and unimplanted areas of a bulk GaAs sample annealed for 60 s at 920 °C. Data from the implanted area reveal a peak at 1.41 eV and a low-energy shoulder just below 1.40 eV, neither of which appear in the unimplanted area or in the Ga^+-implanted control sample. These luminescence features are consistent with previous studies of Mn in bulk GaAs, and originate from closely spaced band-acceptor (e,A^0) and donor-acceptor (D,A^0) transitions, with the low-energy shoulder being a transverse acoustic-phonon replica.[5] Higher implantation doses and/or annealing temperatures and times increase the luminescence intensity, which does not appear to saturate within the parameters of this study. This implies that further integration of Mn ions into the lattice may be possible. In contrast, the implantation energy has little effect on the line shape or intensity, suggesting that the higher beam energies required for high-resolution implantation do not adversely influence ion integration.

Parallel studies in the QW sample reveal significant recovery of the QW ground-state luminescence with annealing and blueshifted luminescence peaks from QW's closest to the surface. Such blueshifting of QW emission is commonly seen in FIB-implanted samples after RTA and results from defect-enhanced Al-Ga interdiffusion across the QW interfaces at elevated temperatures.[6] These shifts are typically several meV, and when combined with a QW stack can be used to monitor lattice damage at different depths. The data are in agreement with previous studies of FIB-implanted Ga^+ (Refs. 6 and 7) and with the Ga^+-implanted control samples.

To examine the magnetic activity of the Mn ions, we investigate the magneto-optical photoluminescence (PL) characteristics of the implanted structures. Samples are arranged in the Faraday configuration within a variable-temperature magneto-optical cryostat and are excited by a linearly polarized model-locked Ti:sapphire laser, whose infrared output is frequency doubled to produce $\sim$100-fs pulses at 2.74 eV. The luminescence spot is directly imaged with a microscope and charge-coupled device detector, enabling easy positioning of the focused laser spot onto the implanted areas. Analysis of the emitted left-handed (σ^-) and right-handed (σ^+) circular polarization intensities (I_-,I_+) is performed with a quarter-wave plate, a rotating half-wave plate, and a linear polarizer. The luminescence is energy resolved to $\sim$0.6 meV using a monochromator and a cooled GaAs photomultiplier tube. Lock-in detection of the modulated signal at $4f$, where

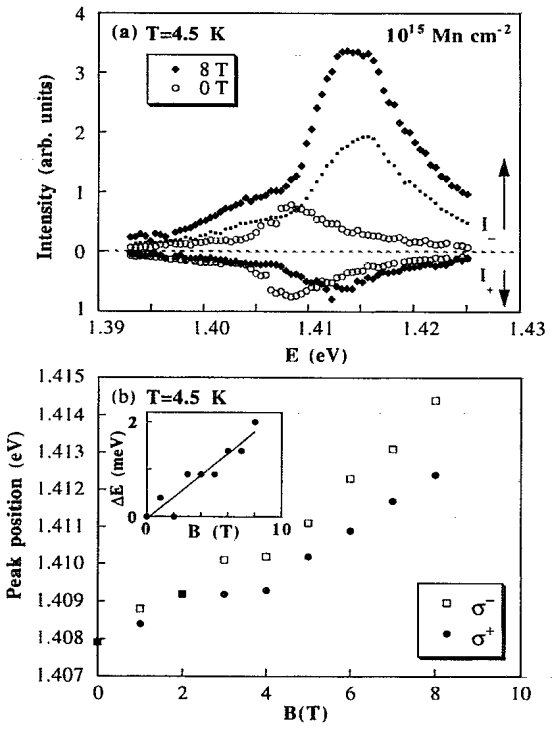

FIG. 2. (a) Polarization-resolved spectra at $B=0$ T (○) and $B=8$ T (◆) from the same implanted area represented in Fig. 1 using 1.1-mW excitation. The dotted line shows power-normalized I_- spectra taken at 7.1 mW and $B=8$ T. (b) Peak positions are shown vs applied field. Laser power is 5 mW, and the resulting Zeeman splitting $\Delta E\equiv E(\sigma^-)-E(\sigma^+)$ is shown in the inset.

f is the rotational frequency of the half-wave plate, generates a signal proportional to the difference signal $I_{\rm diff}=\frac{1}{2}(I_+-I_-)$. Simultaneous lock-in detection at the modulation frequency of the exciting laser provides the average PL signal, $I_{\rm sum}=\frac{1}{2}(I_++I_-)$ and thus a direct measure of the polarization, $P=I_{\rm diff}/I_{\rm sum}$.

As seen in Fig. 2(a), the application of a magnetic field results in a large enhancement of the I_- component of the 1.41-eV emission within an area of the bulk GaAs sample receiving 10^{15} Mn cm^{-2} ($\sim 10^{20}$ Mn cm^{-3} at this implantation energy). Aside from scaling, PL reveals no quantitative differences in the 10^{14} Mn cm^{-2} dosed area, and for lower doses the signal is too weak for comparison. Excitation power dependence from 50 μW to 10 mW reveals that two transitions contribute within the main peak, with the lower-energy peak saturating at lower powers. Figure 2(a) resolves the corresponding change in the line shape for I_- upon increasing power from 1.1 to 7.1 mW. Such behavior supports the assignment of these two peaks as (e,A^0) and (D,A^0) transitions, with the donor-acceptor transition lying about 2 meV lower in energy, in good agreement with earlier work.[5] Figure 2(b) shows the field-dependent peak energy shifts with the Zeeman splitting, $\Delta E\equiv E(\sigma^-)-E(\sigma^+)$, plotted in the inset. Landau quantization of the conduction band should contribute a linear blueshift with field for (e,A^0) transitions, previously measured for dilute Mn in wide GaAs QW's.[8] While the present data are consistent with this prediction, we note that the PL peaks are actually a combination of two

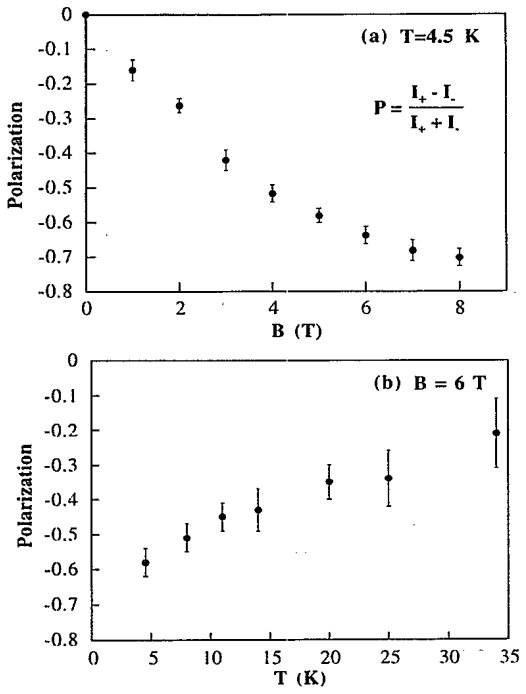

FIG. 3. Polarization vs (a) applied field and (b) temperature for the implanted area represented in Fig. 1.

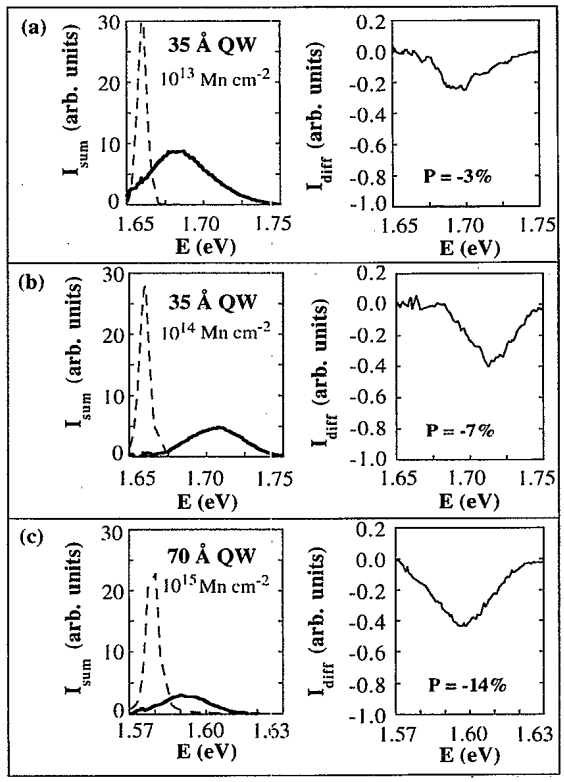

FIG. 4. Difference and sum PL intensities using 1.2 mW in $B=6$ T for 50-keV Mn^{2+} FIB implanted areas of the QW sample annealed at 920 °C for 60 s. Dotted lines indicate the original QW PL spectra, and areal Mn^{2+} dosages are as indicated.

transitions whose relative strengths are a function of the applied field.

The negative sign of the luminescence polarization [Fig. 2(a)] P is atypical when compared to nonmagnetic acceptors in GaAs.[8,9] This may be qualitatively explained by a strong antiferromagnetic spin exchange between a $S=\frac{5}{2}$ Mn acceptor core and a bound $j=\frac{3}{2}$ hole.[8] In this case the usual Zeeman splitting of the $j=\frac{3}{2}$ holes is overcome by the Mn exchange field, leading to a reversal of the hole magnetization and the observed optical polarization. Measurements indicate that in contrast to band-to-band recombination, the polarization is power independent and the closely spaced (e,A^0) and (D,A^0) transitions contributing to the main peak are similarly polarized. These results support our interpretation that the hole spin dictates the optical polarization since polarizations appear relatively insensitive to the electron's initial state.

In contrast to ordinary Zeeman effects, the larger signal comes from the *higher*-energy component (σ^-) over the entire range of excitation power. This counterintuitive result derives from the emitted photon's energy dependence on the *final* spin orientation of the Mn ion. To clarify our discussion, we use a simple model of hole-ion exchange in which the exchange energy dominates the individual Zeeman and thermal energies, so that recombination occurs with a $J \equiv S + j = 1$ neutral acceptor complex.[8,9] In the large $\mu_B B/kT$ limit, recombination of electrons with the lowest energy state, $M_J=-1$, produces both σ^+ and σ^- polarizations. The largest contribution to the σ^- component arises from the recombination of spin-down electrons with $j_z=\frac{3}{2}$ holes, leaving the ionic spin in its lowest energy state, $S_z=-\frac{5}{2}$. In contrast, the σ^+ component emerges with a lower energy since it leaves the Mn ion in an excited state. Although a $J=1$ bound complex with the appropriate g factor of 2.77 has been verified by electron spin resonance for dilute Mn impurities in GaAs,[10,11] we find quantitative discrepancies with our data. This model currently accounts for the sign of the Zeeman effect, but underestimates the magnitude of 0.23 meV/T by $\sim 30\%$.

Figure 3(a) shows the field dependence of the measured polarization which nearly saturates around 70% at $B=8$ T, with a characteristic similar to the Brillouin alignment of paramagnetic Mn ions. The data are in conflict with the simple $J=1$ model and previous measurements of more dilute Mn impurities in GaAs which indicate a lower saturation of the polarization at 50%.[8,9] Differences between light- and heavy-hole masses will modify the spin state of the bound complex, but do not account for discrepancies with previous data. However, the model considered neglects Mn-Mn spin interactions which invalidate the use of J as a good quantum number. It is likely that clusters exist in our highly implanted material, since evidence for Mn clustering has been seen in resonance experiments for concentrations above 5×10^{16} Mn cm^{-3} (Ref. 11) and disorder-enhanced Mn diffusion during annealing would further promote cluster formation. The resulting interactions would affect both the magnitude and temperature dependence of the observed polarizations, especially at temperatures below the Mn-Mn exchange temperature T_{ex}. The strength of the Mn-Mn exchange in GaAs has been inferred from resonance experiments,[11] and show a strong concentration dependence. From these data we esti-

mate a reasonable lower limit for $T_{ex} \sim 4$ K. Furthermore, magnetic susceptibility measurements[12] on samples with 6×10^{18} Mn cm^{-3} indicate that even in the absence of such exchange, one would expect an additional decrease in the polarization above 30 K due to the population of exchange-coupled excited states with $J=2$. Figure 3(b) indicates the measured temperature dependence of the polarization at $B=6$ T.

Studies of the implanted QW sample allow us to see the effects of magnetic impurities in a confined geometry. Band-gap PL measurements taken in the same configuration as the bulk samples reveal a trend toward increasing QW polarization with higher Mn content. Figure 4 shows the sum and difference PL signals at $T=4.5$ K for 50-keV Mn implantation at various doses in $B=6$ T. Average band-gap QW PL spectra outside of (dotted) and within (heavy solid line) the implanted areas demonstrate the variation of the blueshifted QW energy and intensity with dose and depth. Note that the blueshifted peak for the 35-Å well [Figs. 4(a) and 4(b)] produces a larger difference signal at 10^{14} cm^{-2} than at 10^{13} cm^{-2}. Furthermore, at 10^{15} cm^{-2}, though the blueshifted 35-Å well luminescence is not observable, the deeper 70-Å QW is clearly seen [Fig. 4(c)]. A further reduction in this QW PL strength indicating highest Mn content is accompanied by a more polarized emission (14%). Finally, no such trend is evident in the Ga^+-implanted control samples, through similar blueshifted peaks are seen.

In summary, we have developed a method for implanting Mn on submicrometer length scales by FIB. Our results indicate that implanted ions are magnetically active in GaAs, resulting in luminescence polarizations as high as 70% at 8 T. The data also suggest enhanced QW polarization through Mn implantation and illustrate the feasibility of introducing carrier exchange interactions into such structure.

This work was supported by AFOSR Grant No. F49620-93-1-0177, Fujitsu Grant No. 8-442490-46201, and the NSF Science and Technology Center for Quantized Electronic Structures, Grant No. DMR 91-20007.

[1] J. K. Furdyna, J. Appl. Phys. **64**, R29 (1988).
[2] H. Ohno *et al.*, Phys. Rev. Lett. **68**, 2664 (1992).
[3] H. Munekata *et al.*, Phys. Rev. Lett. **63**, 1849 (1989).
[4] M. Tanaka *et al.*, Appl. Phys. Lett. **62**, 1565 (1993).
[5] M. Ilegems, R. Dingle, and L. W. Rupp, Jr., J. Appl. Phys. **46**, 3059 (1975).
[6] F. Laruelle *et al.*, J. Vac. Sci. Technol. B **7**, 2034 (1989).
[7] F. Laruelle *et al.*, Appl. Phys. Lett. **56**, 1561 (1990).
[8] A. Petrou *et al.*, Solid State Commun. **55**, 865 (1985).
[9] I. Y. Karlik *et al.*, Fiz. Tverd. Tela Leningrad **24**, 3550 (1982) [Sov. Phys. Solid State **24**, 2022 (1982)].
[10] J. Schneider *et al.*, Phys. Rev. Lett. **59**, 240 (1987).
[11] V. F. Masterov *et al.*, Fiz. Tekh. Poluprovodn. **17**, 1259 (1983) [Sov. Phys. Semicond. **17**, 796 (1983)].
[12] T. Frey *et al.*, J. Phys. C **21**, 5539 (1988).